

Article

Electro-Reduction of Molecular Oxygen Mediated by a Cobalt(II)octaethylporphyrin System onto Oxidized Glassy Carbon/Oxidized Graphene Substrate

Camila Canales ¹, Leyla Gidi ¹, Roxana Arce ², Francisco Armijo ¹, María J. Aguirre ^{3,*}  and Galo Ramírez ^{1,*}

¹ Departamento de Química Inorgánica, Facultad de Química y de Farmacia, Pontificia Universidad Católica de Chile, Av. Vicuña Mackenna 4860, Casilla 306, Correo 22, Santiago 7820436, Chile; cicanale@uc.cl (C.C.); ldgidi@uc.cl (L.G.); jarmijom@uc.cl (F.A.)

² Departamento Ciencias Biológicas y Químicas, Facultad de Medicina y Ciencia, Universidad San Sebastián, Lota 2465, Providencia, Santiago 7510157, Chile; arce.roxana@gmail.com

³ Departamento de Química de los Materiales, Facultad de Química y Biología, Universidad de Santiago de Chile USACH. Av. L.B. O'Higgins 3363, Santiago 9170019, Chile

* Correspondence: maria.aguirre@usach.cl (M.J.A.); gramirezj@uc.cl (G.R.)

Received: 5 November 2018; Accepted: 3 December 2018; Published: 6 December 2018



Abstract: The oxygen reduction reaction (ORR) is the most important reaction in life processes and in energy transformation. The following work presents the design of a new electrode which is composed by deposited cobalt octaethylporphyrin onto glassy carbon and graphene, where both carbonaceous materials have been electrochemically oxidized prior to the porphyrin deposition. The novel generated system is stable and has an electrocatalytic effect towards the oxygen reduction reaction, as a result of the significant overpotential shift in comparison to the unmodified electrode and to the electrodes used as target. Kinetic studies corroborate that the system is capable of reducing molecular oxygen via four electrons, with a Tafel slope value of 60 mV per decade. The systems were morphologically characterized by scanning electron microscopy (SEM) and atomic force microscopy (AFM) Electrochemical impedance spectroscopy studies showed that the electrode previously oxidized and modified with cobalt porphyrin is the system that possesses lower resistance to charge transfer and higher capacitance.

Keywords: oxygen reduction reaction; glassy carbon electrode; graphene; metalloporphyrins

1. Introduction

The oxygen reduction reaction (ORR) is determinant for the operation of devices associated with the conversion and storage of energy, such as fuel cells and metal–air batteries, among others [1–5]. In this sense, the development of electrocatalysts for ORR becomes crucial both for the use and commercialization of these technologies [6]. Nowadays, the best electrocatalysts for ORR are associated with high cost materials, related to Pt and derived materials, such as Pt nanoparticles onto other low-cost substrates [7–10]. However, the scarcity of this material, as well as the high cost associated with it, means that large-scale applications are very difficult [11,12]. On the other hand, the feasibility of generating low-cost electrocatalysts to reduce molecular oxygen at low overpotentials has been demonstrated. Consequently, this has proved that carbon-based materials, such as activated carbon (carbon black), carbon nanotubes, carbon nanofibers, and graphene, among others, play an important role in overcoming challenges concerning technology, energy, and practical applications. In this regard, these materials have been widely used and are promising in applications of great importance, such as in the generation of energy via electrochemical and electrocatalytic processes [13]. Therefore,

carbonaceous materials, such as glassy carbon (GC) and graphene (GPH), can be excellent choices to be used as electrode substrates [14]. Thus, since graphene-based materials emerged, they have been identified as interesting candidates to be applied as catalysts due to their high conductivity, large surface area, high chemical/electrochemical stability, as well as their strong adherence to compounds with catalytic characteristics [15–17]. In addition, the large quantities of functional groups that an oxidized graphene may contain can provide more active sites for nucleation processes and coordinate catalytic compounds [18]. Thus, several works based on carbonaceous materials have been published, which demonstrate the effectiveness of these systems for multiple reactions of environmental and energy interest [19–23].

On the other hand, several studies are focused on substituting the use of Pt as an electrocatalyst material. In addition, carbonaceous materials allow to reduce costs compared to Pt-based materials, where both GC and GPH have great advantages in terms of cost. Nevertheless, the use of metal complexes (non-noble) has been used in order to generate new electrode systems that are capable of reducing molecular oxygen (e.g., Fe, Ni, Co), where Co(II) complexes have attracted great attention. Among these complexes, aza-macrocyclic type compounds are found, such as phthalocyanines and porphyrins, which possess excellent redox properties [24,25] that make them candidates to modify electrode substrates so as to electrocatalyze multiple reactions, such as oxygen reduction reaction, hydrogen evolution reaction, and carbon dioxide reduction, which are important reactions in the area of energy generation and storage. Additionally, multiple electrode systems have been generated using this type of complexes [26–29], which allows the obtainment of significant potential shifts and high efficiencies towards ORR. Previously, our group reported a very electrocatalytic system, which was capable of reducing molecular oxygen via four electrons using a commercial octaethylated cobalt porphyrin onto oxidized GC. In that study, it was found that oxidized groups serve as anchoring molecules that permit the coordination of a first layer of metalloporphyrin and provide stability to the system [30]. After the coordination of the first layer, the porphyrins are then arranged in a columnar side-to-side form over the covalently modified system, as demonstrated by RAMAN spectroscopy, X-ray diffraction (XRD), and UV-Vis spectroscopy [31,32].

Finally, considering the abovementioned background, this paper presents the generation of a simple and active GC/GPH/Co(II)EPO system (Figure 1), where carbon materials are previously oxidized at a fixed potential (+1.6 V versus Ag/AgCl and +1.0 versus Ag/AgCl for GC and GPH, respectively). Oxidized groups are generated on the surface in order to serve as anchoring molecules to coordinate the first layer of cobalt porphyrins. In this way, it is expected that the system could aid as an electrocatalyst towards the molecular oxygen reduction reaction as a result of the contribution of glassy carbon, graphene, oxidized groups, and cobalt porphyrin, in a synergistic way. Concomitantly, the existence of these anchoring molecules is expected to stabilize the generated system, so as to have stable and reproducible responses over time.

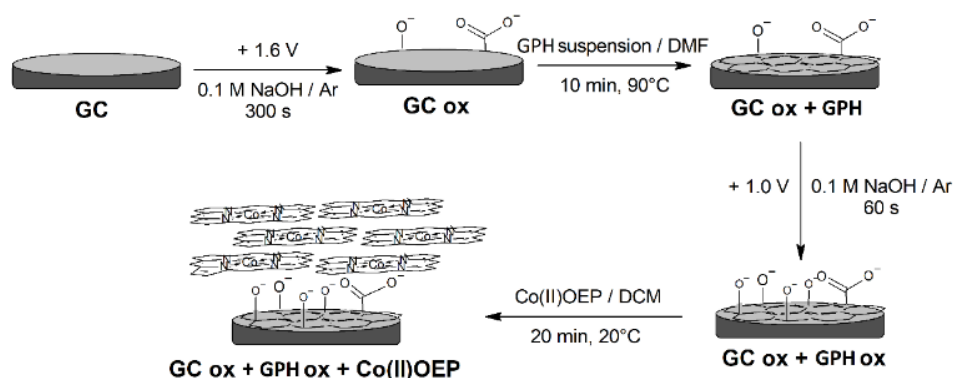


Figure 1. Modification diagram of vitreous carbon electrode (GC = Glassy Carbon, ox = oxidized, GPH = Graphene, Co(II)OEP = cobalt(II)octaethylporphine, DFM = dimethylformamide, DCM = dichloromethane).

2. Results and Discussion

2.1. Morphological Studies of Modified Systems

In order to study the systems in terms of morphology, SEM studies were conducted for the GC, GC + GPH, GC ox + GPH ox, and GC ox + GPH ox + Co(II)EPO systems. Figure 2 shows the images corresponding to these studies. As observed, noticeable differences exist in comparison to the surface morphologies presented by each system.

The addition of GPH onto the GC substrate causes the dispersion of GPH agglomerations along the entire surface of the electrode. However, when the GPH is deposited on previously oxidized GC (GC ox + GPH), and also when the GC ox + GPH ox system is subsequently generated, many more covered substrates are obtained, with larger agglomerations than those observed by the non-oxidized GC + GPH system.

Finally, it is possible to observe how the metallic cobalt porphyrin deposits change the morphology of the electrode system, owing to the appearance of fibers on the oxidized surface. It is noteworthy that these porphyrin deposits are mostly arranged on the agglomerations rather than on the unmodified surface, which corroborates that the oxidized groups help the metal complex to be coordinated to the system more easily. On the other hand, AFM images, shown next to each SEM image, complement the morphological analysis of the resulting surfaces in terms of roughness (R_q) variation. As can be seen, the initial GC substrate has a R_q value of 6.0 nm, being the lowest in comparison to the modified systems whose R_q have values of up to 355.0 nm (Table 1). In this regard, the modified system GC ox + GPH ox + Co(II)OEP presents the highest roughness value in comparison to the rest of the systems, which would explain the increment in both the capacitance of the system and the total current, as will be seen later. At the same time, the formation of agglomerations is observed, which may indicate the formation of columnar systems given the nature of porphyrin complexes that have the ability to be arranged one over another through π -stacking [30].

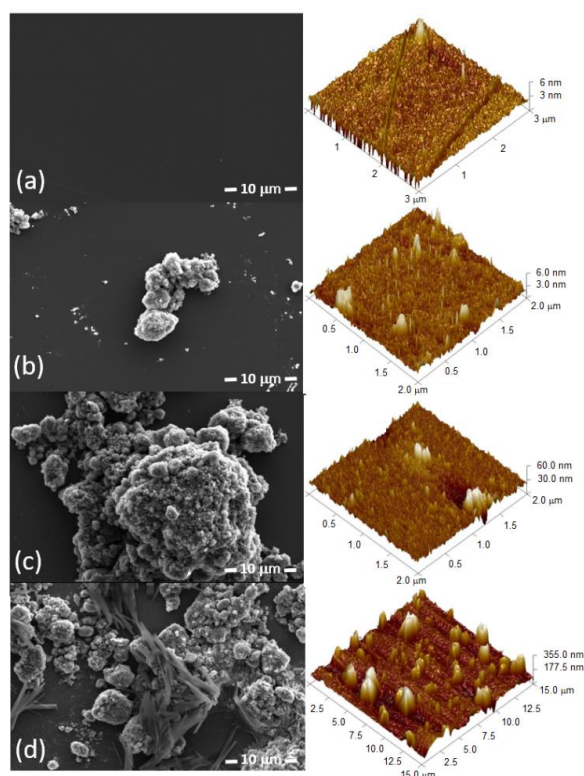


Figure 2. Morphological studies by SEM (left) and AFM (right) for (a) GC, (b) GC + GPH, (c) GC ox + GPH ox and (d) GC ox + GPH ox + Co(II)OEP systems.

Table 1. R_q values for the GC systems and modified GC systems.

System	R_q (nm)
GC	6.0
GC + GPH	6.0
GC ox + GPH ox	60.0
GC ox + GPH ox + Co(II)OEP	355.0

2.2. Electrochemical Response of the Modified Systems

Figure 3a shows the voltammetric responses of GC, GC + GPH, GC + GPH + Co(II)EPO, GC ox + GPH ox, and GC ox + GPH ox + Co(II)EPO systems. As shown in Figure 3a, all the modified systems have a different voltammetric profile and potential shifts compared to the initial substrate. In this regard, a significant shift on the onset potential of 400 mV appears compared to the GC, associated to the GC ox + GPH ox + Co(II)OEP system, which, in turn, presents a significant current increment, which reaches a cathodic peak current of 80 μ A. Consequently, it is possible to demonstrate the synergistic effect between the oxidized carbonaceous materials (GC ox + GPH ox) and the porphyrin cobalt complex (Co(II)OEP), since, in the first case, the potential shift of the onset potential is small in comparison to the ones shown by the initial substrates (GC + GPH). However, after the deposition of the cobalt complex, both GC + GPH + Co(II)OEP and GC ox + GPH ox + Co(II)OEP systems present significant onset potential shifts, due to the contribution of the metallic complex, as has been demonstrated in previous works with similar systems [30,33–35]. This phenomenon is typical in electrode systems that are modified with cobalt-containing compounds, such as cobalt oxide (II, III), Co_3O_4 [36,37]. It is remarkable that the porphyrin complex deposited on the GC modified with non-oxidized GPH is substantially less catalytic than the system shown here, where both carbonaceous substrates have been previously oxidized. This result draws attention because graphene oxidation should bring about a conductivity loss associated with the loss of sp^2 hybridization that is not observed in the results here obtained. By contrast, oxidized carbonaceous and non-oxidized materials show a similar profile for the oxygen reduction, with the same onset potentials. In this sense, it is important to highlight this latter effect: The manifested synergy between the Co(II)OEP and carbon-based materials is much greater when the carbonaceous materials are previously oxidized.

Thus, the porphyrin-modified oxidized system has the greatest electrocatalytic effect towards ORR, reducing molecular oxygen to an onset potential of -0.08 V.

As well as the faradaic current increases in the GC ox + GPH ox + Co(II)OEP system, the capacitive current also presents a high increment in comparison to the bare GC (Figure 3b).

The existence of oxidized groups that serve as covalent anchoring groups to the first layer of deposited porphyrins generates an increment in the number of components on the electrode surface, which results in the double layer increment (capacitance) and, therefore, in the capacitive current presented by the modified system [38].

On the other hand, as seen in Figure 3b, the modified system shows a slight anodic signal at ca. 0.0 V, associated to the Co(II)/Co(III) redox couple. Thus, the generation of μ -oxo bonding is formed by the porphyrin central metal, which implies the formation of oxidized cobalt species that facilitates, finally, the molecular oxygen reduction [39].

By contrast, the existence of oxidized graphene provokes a synergistic effect on the electrodic system, by increasing the electrocatalytic effect that the GC ox + Co(II)OEP system already possesses, as reported in a previous work of our group [30]. Thus, the existence of oxidized graphene (GPH ox) is crucial to achieve a greater electrocatalytic effect and the addition of robustness to the modified electrode.

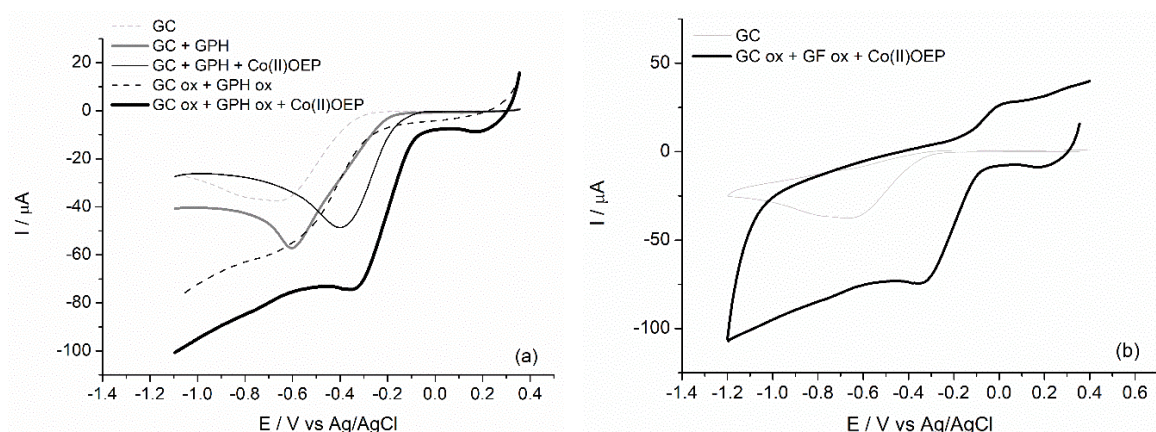


Figure 3. (a) Voltammetric profiles of all studied systems, (b) cyclic voltammetry profiles for GC and GC ox + GPH ox + Co(II)OEP systems, in 0.1 M NaOH saturated with O₂. $v = 0.1 \text{ Vs}^{-1}$.

2.3. Electrochemical Kinetics

In order to know how ORR occurs at the electrode–solution interphase, the corresponding kinetic study of the GCox + GPH ox + Co(II) OEP system was conducted. Figure 4a shows the linearity of the logarithm of the peak current ($\log I_p$) vs. logarithm of the scan rate ($\log v$), which gives a slope value of 0.48 (~0.5) that implies that the ORR process is diffusion-controlled [40]. Figure 4b depicts the variation of the peak current vs. the square root of the scan rate, which affords a linear plot ($R^2 = 0.998$); these results are consistent with the diffusion-controlled process.

This background enables the determination of the number of transferred electrons, n , during the reduction reaction using the Randles–Sevcik equation (Equation (1)) for irreversible diffusion-controlled systems, such as the one shown in this case [40,41]. In this equation, α is the charge transfer coefficient, n_a the number of electrons involved in the rate-determining step of the reaction, D_0 ($2 \times 10^{-5} \text{ cm}^2 \text{ s}^{-1}$) [42] the diffusion coefficient of the electroactive specie, and C_0 , the concentration of O₂ on the solution, which corresponds to $6.90 \times 10^{-7} \text{ mol cm}^{-3}$ in O₂ saturated aqueous solutions at room temperature [43].

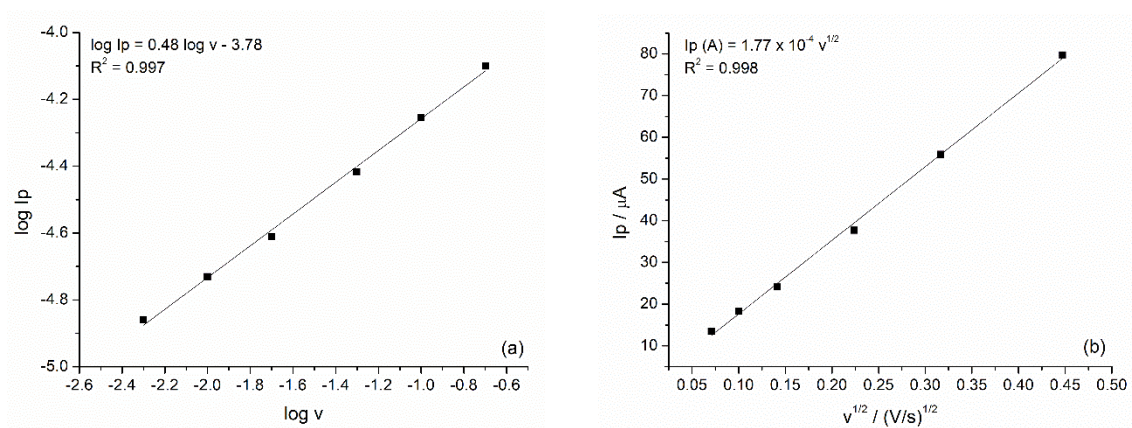


Figure 4. Kinetic studies. (a) Dependence of the logarithm of the peak current on scan rate logarithm. (b) Dependence of peak current on square-root of scan rate.

Then, considering the information given in Figure 4 and the Randles–Sevcik equation (Equation (1)) described above, it is possible to infer that:

$$I_p = (2.99 \times 10^5) n [(1 - \alpha)n_a]^{1/2} C_0 A D_0^{1/2} v^{1/2} \quad (1)$$

$$\frac{I_P}{v^{1/2}} = 177 \times 10^{-6} \text{ A} (\text{Vs}^{-1})^{-1/2} \quad (2)$$

$$\frac{I_P}{v^{1/2}} = (2.99 \times 10^5) n [(1 - \alpha)n_a]^{1/2} 6.90 \times 10^{-7} \text{ mol cm}^{-3} 0.070 \text{ cm}^2 (2 \times 10^{-5} \text{ cm}^2 \text{ s}^{-1})^{1/2} \quad (3)$$

$$177 \times 10^{-6} \text{ A} (\text{Vs}^{-1})^{-1/2} = (6.46 \times 10^{-5}) n [(1 - \alpha)n_a]^{1/2} \quad (4)$$

$$2.7 = n [(1 - \alpha)n_a]^{1/2} \quad (5)$$

Furthermore, considering that $(1 - \alpha)n_a$ must be known, an equation based on its dependence on the difference between the peak potential (E_p) and the half-peak potential ($E_{p/2}$) was employed as follows [44]:

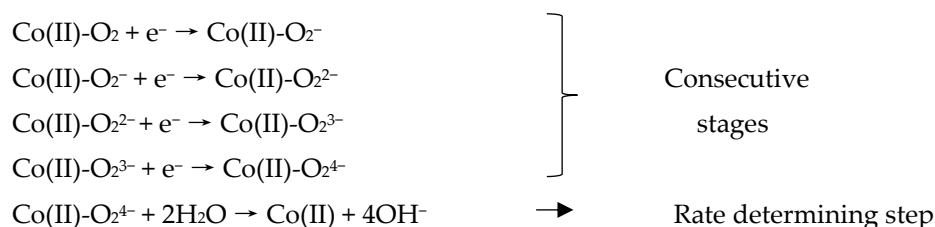
$$(1 - \alpha)n_a = 0.0477 \text{ V} / |(-0.332 \text{ V} + 0.184 \text{ V})| = 0.32 \quad (6)$$

$$[(1 - \alpha)n_a]^{1/2} = 0.6 \quad (7)$$

$$n = \frac{2.7}{0.6} = 4.6 \text{ electrons} \quad (8)$$

Finally, the trend of the system to reduce the electroactive species via four electrons is demonstrated.

Concomitantly, the Tafel slope for the proposed system was calculated. Figure 5 shows the obtained plot at low overpotentials, which gives a slope value of $2.303RT/\alpha F \approx 60 \text{ mV}$ per decade that corresponds to a chemical step subsequent to the first electronic transfer, as the rate-determining step of the reaction (Rds) [45]. In this sense, there would be a direct oxygen reduction reaction involving four electrons, where the first electronic transfer is followed by the breaking of the double O–O bond, which would comprise the slow step, without the formation of peroxide intermediates [46–48]. Consequently, the following mechanism may be proposed:



This mechanism includes the previous stage of an adduct formation between the metallic center and the oxygen, adduct where internal charge transfer from the metallic center to the oxygen can take place, which is not included in the above-shown mechanism in order to simplify the steps. In the four-electron transfer, the Co metal center behaves as an electronic bridge that would transfer the charge towards the oxygen bond, until this molecule receives four electrons. These first four stages would occur consecutively, at very close potentials, which give rise to a single, rather wide, cathodic wave (Figure 3b) due to the small differences in energy that each electron transfer requires. At that point, considering these four fast steps and close in energy, the rate determining step would comprise the reaction of the negative charged adduct with water from the medium to break up, generating hydroxyl ions as final products.

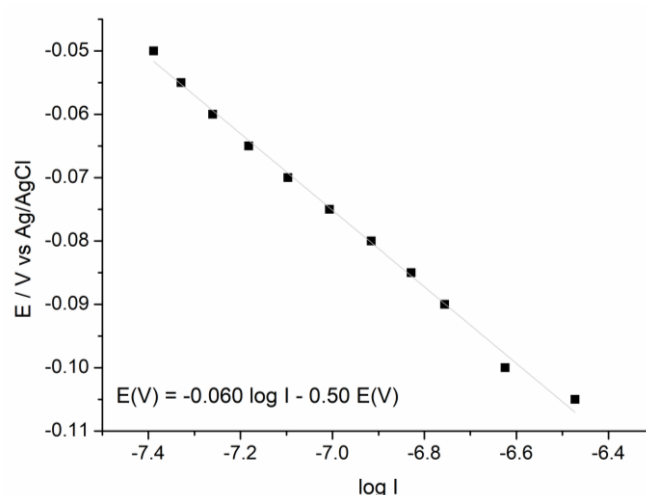


Figure 5. Potential dependence on current logarithm (Tafel slope), for the GC ox + GPH ox + Co(II)OEP system.

Finally, in order to corroborate the stability of the generated system, chronoamperometry was performed at fixed potential during 3600 s. As appreciated in Figure 6, the system attains a current response that remains constant over time, evidencing that the system, as well as being efficient and easy to obtain, is stable.

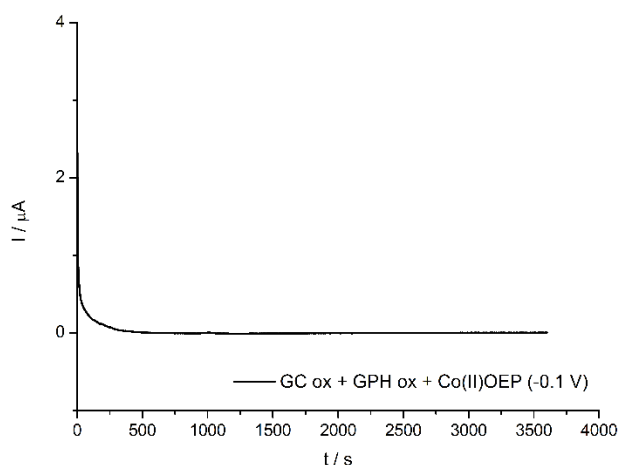


Figure 6. Chronoamperometric study of the GC ox + GPH ox + Co(II)OEP system stability.

2.4. Electrochemical Impedance Spectroscopy

Figure 7 shows the Nyquist diagram for the GC, GC ox + GPH ox, and GC ox + GPH ox + Co(II)OEP systems, obtained at a fixed potential of -0.4 V. The equivalent circuit, whose parameters are summarized in Table 2, is also shown. R_s is the solution resistance, while R_{ct} and CPE are the charge transfer resistance and the constant phase element, respectively.

As is observed, both modified systems, GC ox + GPH ox and GC ox + GPH ox + Co(II)OEP, show a great decrease of charge transfer resistance, graphically associated to the semicircle closure. The GC ox + GPH ox + Co(II)OEP system is the one with the lowest charge transfer resistance, which is consistent with that obtained in the voltammetric studies, which were previously accomplished.

In the equivalent circuit, a constant phase element (CPE) associated with two parameters (T and P) was used. It is assumed that if P is close to 1, T corresponds to the capacitance. If P is close to 0.5, T is associated with diffusion species, whereas if P is close to 0, T will be a resistance value [49]. Table 2 shows the results obtained for this experiment and it can be observed that, in all cases, the

parameter associated with P is close to 1, indicating that T would yield capacitance values, which are higher when rusted systems are used. In addition, it is noteworthy that for oxidized systems, the capacitance value is similar before and after the porphyrin addition. Consequently, it was corroborated that the final obtained capacitance is highly influenced by the oxidized groups in the GC and GPH, respectively, rather than by the presence of the porphyrin complex. Additionally, it can be observed that the diminution of the R_{ct} value is consistent with the electrocatalytic activity, which is given by the overpotential onset value. Concomitantly, the system obtained by GC ox + GPH ox + Co(II)OEP is the most conductive, which evidences its electrocatalytic effect towards ORR.

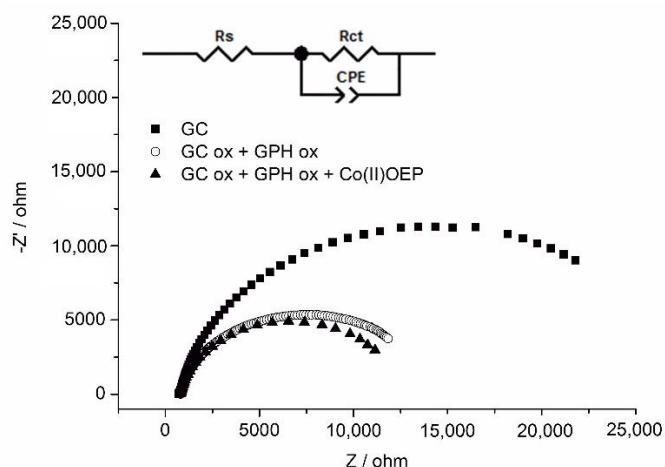


Figure 7. Nyquist plot and equivalent circuit used for GC, GC ox + GPH ox, and GC ox + GPH ox + Co(II)OEP systems, in O_2 -saturated 0.1 M NaOH solution at $E = -0.4$ V, frequency range 0.1–100,000 Hz.

Table 2. Parameters obtained with the equivalent circuit of Figure 7. E_0 is the onset potential, R_s is solution resistance, R_{ct} the charge transfer resistance, and CPE the constant phase element.

System	E_0 (V)	R_s (Ω)	R_{ct} (Ω)	CPE (T, P) (s^{-1})
GC	−0.34	742.1	27,244	3.53×10^{-6} , 0.88
GC ox + GPH ox	−0.25	810.9	12,999	5.20×10^{-6} , 0.88
GC ox + GPH ox + Co(II)OEP	−0.08	796.1	11,905	5.22×10^{-6} , 0.88

Finally, Table 3 compares the generated material (GC ox + GPH ox + Co(II)OEP) with other similar systems that have been previously reported in the literature towards the ORR. In this sense, the electrode here developed is found to be one of the most electroactive systems due to its onset overpotential. Moreover, this new material is easily achieved, highly stable, and cheap.

Table 3. Comparison between similar systems towards the oxygen reduction reaction (ORR).

Material	Medium	ORR Onset (V)	Number Electrons ORR	Reference
GC/GPH	0.1 M KOH	−0.18 vs. SCE	≈ 4	[50]
Cu foil/GPH	0.1 M KOH	−0.3 vs. Ag/AgCl	≈ 2	[51]
GC/GPH Quantum Dots	0.1 M KOH	−0.16 vs. Ag/AgCl	3.6–4.4	[52]
CoTPyP/PSS-rGO *	0.1 M KOH	−0.15 vs. Ag/AgCl	3.61–3.67	[53]
CoP-CMP800 **	0.1 M KOH	−0.1 vs. Ag/AgCl	3.83–3.86	[26]
GC Co(II)OEP	0.1 M NaOH	−0.2 vs. Ag/AgCl	-	[54]
GC Co(II)OEP-Fe(III)OEP	0.1 M NaOH	−0.13 vs. Ag/AgCl	≈ 4	[54]
GC ox/Co(II)OEP	0.1 M NaOH	+0.05 vs. Ag/AgCl	≈ 4	[30]
GC ox + GPH ox + Co(II)OEP	0.1 M NaOH	−0.08 vs. Ag/AgCl	≈ 4	This work

* Cobalt porphyrin on poly(sodium-pstyrenesulfonate) modified reduced graphene oxide. ** Cobalt porphyrin-based conjugated mesoporous polymers.

3. Materials and Methods

3.1. Equipment

Cyclic Voltammetry (CV), chronoamperometry, and electrochemical impedance spectroscopy (EIS) studies were accomplished on a CH Instrument 750D potentiostat galvanostat (Austin, USA). A conventional three-electrode system consisting of a glassy carbon working electrode, a large area platinum wire counter electrode, and Ag/AgCl (3 M, KCl) reference electrode was used for all the measurements. All potentials quoted in this work are relative to this reference electrode.

3.2. Reagents

Potassium chloride, sodium hydroxide, and graphene nanoplatelets were purchased from Merck (Darmstadt, Germany). De-ionized water was obtained from a Millipore-Q system (Darmstadt, Germany) (18.2 M Ω ·cm). Argon (99.99% pure) and dioxygen gas (99.99% pure) were purchased from Linde Chile (Santiago, Chile). Cobalt porphyrin (2,3,7,8,12,13,17,18-octaethyl-21H,23H-porphine cobalt(II)) as well as dichloromethane (DCM, HPLC grade) and dimethylformamide (99.90% DMF) were purchased from J.T. Baker (USA).

3.3. Preparation of Modified Electrodes

The glassy carbon electrode was polished to a mirror finish on a felt pad using alumina slurries (3 μ m), sonicated for 120 s to remove the excess of alumina and finally, cycling the potential between -0.7 V and 0.7 V in a 0.1 M NaOH solution (Ar atmosphere) until stabilization of the electrode response (20 cycles).

To obtain the GC + GPH system, a drop of 0.5 mg·mL $^{-1}$ of graphene suspension (5 mg in 10 mL of dimethylformamide) was placed onto the clean (not oxidized) GC surface, and dried at 95 °C for 10 min to evaporate the excess of dimethylformamide (DMF).

The oxidized GC (GC ox) was obtained by applying a constant anodic potential ($+1.6$ V) until the system accumulated a charge of 0.1 C (300 s approximately) in 0.1 M NaOH. Then, one drop of the graphene suspension was placed upon the GC ox surface and dried as aforementioned. After that procedure, a constant anodic potential ($+1.0$ V) was again applied for 60 s, in order to generate the GC ox + GPH ox system. Finally, the obtained system was immersed into a metalloporphyrin solution, M-OEP (M = Co(II)) 0.2 mM dissolved in CH₂Cl₂ for 20 min and finally dried at room temperature for 1 minute (GC ox + GPH ox + Co(II)OEP). To obtain the GC + GPH + Co(II)OEP blank system, the oxidation procedure was omitted. The electrodes were rinsed with fresh deionized water after each modification step.

3.4. Instrumentation

All modified electrodes were analyzed using CV in a 0.1 M NaOH solution saturated with dioxygen (bubbling during 20 min before each measurement) by cycling the potential from 0.4 to -1.1 V.

Chronoamperometry was conducted in a 0.1 M NaOH solution saturated with dioxygen. The modified electrode was tested by measuring the current at a constant potential of -0.1 V for 1000 s.

Electrochemical impedance spectroscopy (EIS) was performed at a constant potential of -0.4 V in a 0.1 M NaOH solution saturated with dioxygen at frequencies that range between 0.1 and $100,000$ Hz.

The scanning electron microscopy studies were carried out on a SEM LEO 1420 VP equipment (Cambridge, England).

4. Conclusions

In the current work, a new system consisting of cobalt octaethylporphyrin on glassy carbon and graphene was obtained; both carbonaceous materials have been previously electrochemically oxidized to carry out the porphyrin deposition of (GC ox + GPH ox + Co(II)OEP). In addition to

being stable, this system exhibited the ability to electrocatalyze the ORR via four electrons, showing a large potential shift towards positive values in relation to independent substrates, unoxidized or oxidized, and without porphyrin deposit. This new material presents a Tafel slope of 60 mV per decade, indicating that is a fast kinetic system, where the rate determining step corresponds to a chemical one. The studies conducted using electrochemical impedance showed that this novel system possesses lower charge transfer resistance, as well as a higher capacitance compared to glassy carbon and oxidized carbonaceous substrates.

Author Contributions: C.C. and L.G. performed the experiments. R.A. and F.A. investigated the relevant literature and helped to write this manuscript. M.J.A. and G.R. wrote, reviewed, and modified this manuscript. All authors contributed to the general discussion about this work.

Funding: This research received no external funding.

Acknowledgments: This work was supported by FONDECYT Project No.: 1170340; FONDECYT Project N° 1160324; Dicyt-Usach, and Doctoral Scholarship CONICYT Project No.: 21170542.

Conflicts of Interest: The authors declare no conflict of interest.

References

1. Jiang, W.J.; Gu, L.; Li, L.; Zhang, Y.; Zhang, X.; Zhang, L.J.; Wang, J.Q.; Hu, J.S.; Wei, Z.; Wan, L.J. Understanding the high activity of Fe-N-C electrocatalysts in oxygen reduction: Fe/Fe₃C nanoparticles boost the activity of Fe-N(x). *J. Am. Chem. Soc.* **2016**, *138*, 3570–3578. [[CrossRef](#)] [[PubMed](#)]
2. Geng, D.; Chen, Y.; Chen, Y.; Li, Y.; Li, R.; Sun, X.; Ye, S.; Knights, S. High oxygen-reduction activity and durability of nitrogen-doped graphene. *Energy Environ. Sci.* **2011**, *4*, 760–764. [[CrossRef](#)]
3. Steele, B.C.; Heinzel, A. Materials for fuel-cell technologies. *Nature* **2001**, *414*, 345–352. [[CrossRef](#)] [[PubMed](#)]
4. Liang, H.W.; Zhuang, X.; Bruller, S.; Feng, X.; Mullen, K. Hierarchically porous carbons with optimized nitrogen doping as highly active electrocatalysts for oxygen reduction. *Nat. Commun.* **2014**, *5*, 4973. [[CrossRef](#)]
5. Van der Vliet, D.F.; Wang, C.; Tripkovic, D.; Strmcnik, D.; Zhang, X.F.; Debe, M.K.; Atanasoski, R.T.; Markovic, N.M.; Stamenkovic, V.R. Mesostructured thin films as electrocatalysts with tunable composition and surface morphology. *Nat. Mater.* **2012**, *11*, 1051–1058. [[CrossRef](#)] [[PubMed](#)]
6. Zhou, T.; Ma, R.; Zhou, Y.; Xing, R.; Liu, Q.; Zhu, Y.; Wang, J. Efficient N-doping of hollow core-mesoporous shelled carbon spheres via hydrothermal treatment in ammonia solution for the electrocatalytic oxygen reduction reaction. *Microporous Mesoporous Mater.* **2018**, *261*, 88–97. [[CrossRef](#)]
7. Alia, S.M.; Jensen, K.; Contreras, C.; Garzon, F.; Pivovar, B.; Yan, Y. Platinum coated copper nanowires and platinum nanotubes as oxygen reduction electrocatalysts. *ACS Catal.* **2013**, *3*, 358–362. [[CrossRef](#)]
8. Narayanamoorthy, B.; Datta, K.K.R.; Eswaramoorthy, M.; Balaji, S. Improved oxygen reduction reaction catalyzed by Pt/Clay/naion nanocomposite for PEM fuel cells. *ACS Appl. Mater. Interfaces* **2012**, *4*, 3620–3626. [[CrossRef](#)]
9. Zhang, Y.; Han, T.; Fang, J.; Xu, P.; Li, X.; Xu, J.; Liu, C.-C. Integrated Pt₂Ni alloy@Pt core-shell nanoarchitectures with high electrocatalytic activity for oxygen reduction reaction. *J. Mater. Chem. A* **2014**, *2*, 11400–11407. [[CrossRef](#)]
10. Zhao, R.; Liu, Y.; Liu, C.; Xu, G.; Chen, Y.; Tang, Y.; Lu, T. Pd@Pt core-shell tetrapods as highly active and stable electrocatalysts for the oxygen reduction reaction. *J. Mater. Chem. A* **2014**, *2*, 20855–20860. [[CrossRef](#)]
11. Gasteiger, H.A.; Kocha, S.S.; Sompalli, B.; Wagner, F.T. Activity benchmarks and requirements for Pt, Pt-alloy, and non-Pt oxygen reduction catalysts for PEMFCs. *Appl. Catal. B Environ.* **2005**, *56*, 9–35. [[CrossRef](#)]
12. Chen, A.; Holt-Hindle, P. Platinum-based nanostructured materials: Synthesis, properties, and applications. *Chem. Rev.* **2010**, *110*, 3767–3804. [[CrossRef](#)] [[PubMed](#)]
13. You, P.Y.; Kamarudin, S.K. Recent progress of carbonaceous materials in fuel cell applications: An overview. *Chem. Eng. J.* **2017**, *309*, 489–502. [[CrossRef](#)]
14. Chabot, V.; Higgins, D.; Yu, A.; Xiao, X.; Chena, Z.; Zhang, J. A review of graphene and graphene oxide sponge: Material synthesis and applications to energy and the environment. *Energy Environ. Sci.* **2014**, *7*, 1564–1596. [[CrossRef](#)]
15. Liang, Y.; Li, Y.; Wang, H.; Zhou, J.; Wang, J.; Regier, T.; Dai, H. Co₃O₄ nanocrystals on graphene as a synergistic catalyst for oxygen reduction reaction. *Nat. Mater.* **2011**, *10*, 780–786. [[CrossRef](#)] [[PubMed](#)]

16. Zhou, W.; Ge, L.; Chen, Z.-G.; Liang, F.; Xu, H.-Y.; Motuzas, J.; Julbe, A.; Zhu, Z. Amorphous iron oxide decorated 3D heterostructured electrode for highly efficient oxygen reduction. *Chem. Mater.* **2011**, *23*, 4193–4198. [[CrossRef](#)]
17. Wu, J.; Zhang, D.; Wang, Y.; Wan, Y.; Hou, B. Catalytic activity of graphene–cobalt hydroxide composite for oxygen reduction reaction in alkaline media. *J. Power Sources* **2012**, *198*, 122–126. [[CrossRef](#)]
18. Bai, H.; Li, C.; Shi, G. Functional composite materials based on chemically converted graphene. *Adv. Mater.* **2011**, *23*, 9, 1089–1115. [[CrossRef](#)]
19. Alenezi, K. Electrocatalytic Hydrogen Evolution Reaction Using mesotetrakis-(pentafluorophenyl)porphyrin iron(III) chloride. *Int. J. Electrochem. Sci.* **2017**, *12*, 812–818. [[CrossRef](#)]
20. Guo, D.; Shibuya, R.; Akiba, C.; Saji, S.; Kondo, T.; Nakamura, J. Active sites of nitrogen-doped carbon materials for oxygen reduction reaction clarified using model catalysts. *Science* **2016**, *351*, 361–365. [[CrossRef](#)]
21. Belova, A.I.; Kwabi, D.G.; Yashina, L.V.; Shao-Horn, Y.; Itkis, D.M. Mechanism of Oxygen Reduction in Aprotic Li–Air Batteries: The Role of Carbon Electrode Surface Structure. *J. Phys. Chem. C* **2017**, *121*, 1569–1577. [[CrossRef](#)]
22. Zhou, M.; Wang, H.-L.; Guo, S. Towards high-efficiency nanoelectrocatalysts for oxygen reduction through engineering advanced carbon nanomaterials. *Chem. Soc. Rev.* **2016**, *45*, 1273–1307. [[CrossRef](#)] [[PubMed](#)]
23. Wang, H.; Min, S.; Wang, Q.; Li, D.; Casillas, G.; Ma, C.; Li, Y.; Liu, Z.; Li, L.-J.; Yuan, J.; et al. Nitrogen-Doped Nanoporous Carbon Membranes with Co/CoP Janus-Type Nanocrystals as Hydrogen Evolution Electrode in Both Acidic and Alkaline Environments. *ACS Nano* **2017**, *11*, 4358–4364. [[CrossRef](#)] [[PubMed](#)]
24. Zagal, J.H.; Bedioui, F. *Electrochemistry of N4 Macrocyclic Metal Complexes: Volume 2: Biomimesis, Electroanalysis and Electrosynthesis of MN4 Metal Complexes*; Springer: Berlin, Germany, 2016.
25. Manbeck, G.F.; Fujita, E. A review of iron and cobalt porphyrins, phthalocyanines and related complexes for electrochemical and photochemical reduction of carbon dioxide. *J. Porphyr. Phthalocyanines* **2015**, *19*, 45–46. [[CrossRef](#)]
26. Wu, Z.-S.; Chen, L.; Liu, J.; Parvez, K.; Liang, H.; Shu, J.; Sachdev, H.; Graf, R.; Feng, X.; Müllen, K. High-Performance Electrocatalysts for Oxygen Reduction Derived from Cobalt Porphyrin-Based Conjugated Mesoporous Polymers. *Adv. Mater.* **2014**, *26*, 1450–1455. [[CrossRef](#)] [[PubMed](#)]
27. Chatterjee, S.; Sengupta, K.; Mondal, B.; Dey, S.; Dey, A. Factors Determining the Rate and Selectivity of $4e^-/4H^+$ Electrocatalytic Reduction of Dioxygen by Iron Porphyrin Complexes. *Acc. Chem. Res.* **2017**, *50*, 1744–1753. [[CrossRef](#)] [[PubMed](#)]
28. Hu, X.-M.; Salmi, Z.; Lillethorup, M.; Pedersen, E.B.; Robert, M.; Pedersen, S.U.; Skrydstrup, T.; Daasbjerg, K. Controlled electropolymerisation of a carbazole-functionalised iron porphyrin electrocatalyst for CO₂ reduction. *Chem. Commun.* **2016**, *52*, 5864–5867. [[CrossRef](#)]
29. Hod, I.; Farha, O.K.; Hupp, J.T. Electrocatalysis: Powered by porphyrin packing. *Nat. Mater.* **2015**, *14*, 1192–1193. [[CrossRef](#)]
30. Canales, C.; Ramírez, G. Glassy carbon electrodes modified with supramolecular assemblies generated by p-stacking of Cobalt (II) octaethylporphyrins. A 4 electrons-dioxygen reduction reaction occurring at positive potentials. *Electrochim. Acta* **2015**, *173*, 636–641. [[CrossRef](#)]
31. Canales, C.; Varas-Concha, F.; Mallouk, T.E.; Ramírez, G. Enhanced electrocatalytic hydrogen evolution reaction: Supramolecular assemblies of metalloporphyrins on glassy carbon electrodes. *Appl. Catal. B Environ.* **2016**, *188*, 169–176. [[CrossRef](#)]
32. Canales, C.; Olea, A.F.; Gidi, L.; Arce, R.; Ramírez, G. Enhanced light-induced hydrogen evolution reaction by supramolecular systems of cobalt(II) and copper(II) octaethylporphyrins on glassy carbon electrodes. *Electrochim. Acta* **2017**, *258*, 850–857. [[CrossRef](#)]
33. Tang, H.; Yin, H.; Wang, J.; Yang, N.; Wang, D.; Tan, Z. Molecular Architecture of Cobalt Porphyrin Multilayers on Reduced Graphene Oxide Sheets for High-Performance Oxygen Reduction Reaction. *Angew. Chem.* **2013**, *125*, 5695–5699. [[CrossRef](#)]
34. Jiang, R.; Chu, D. Comparative study of CoFeNx/C catalyst obtained by pyrolysis of hemin and cobalt porphyrin for catalytic oxygen reduction in alkaline and acidic electrolytes. *J. Power Sources* **2014**, *245*, 352–361. [[CrossRef](#)]
35. Oldacre, A.N.; Friedman, A.E.; Cook, T.R. A Self-Assembled Cofacial Cobalt Porphyrin Prism for Oxygen Reduction Catalysis. *J. Am. Chem. Soc.* **2017**, *139*, 1424–1427. [[CrossRef](#)] [[PubMed](#)]

36. Ma, T.Y.; Dai, S.; Jaroniec, M.; Qiao, S.Z. Metal–Organic Framework Derived Hybrid Co₃O₄-Carbon Porous Nanowire Arrays as Reversible Oxygen Evolution Electrodes. *J. Am. Chem. Soc.* **2014**, *136*, 13925–13931. [[CrossRef](#)] [[PubMed](#)]
37. Zhuang, Z.; Sheng, W.; Yan, Y. Synthesis of Monodisperse Au@Co₃O₄ Core-Shell Nanocrystals and Their Enhanced Catalytic Activity for Oxygen Evolution Reaction. *Adv. Mater.* **2014**, *26*, 3950–3955. [[CrossRef](#)] [[PubMed](#)]
38. Scholz, F. (Ed.) *Electroanalytical Methods: Guide to Experiments and Applications*; Springer: Berlin, Germany, 2013; ISBN 3662047578, 9783662047576.
39. Marín, A.; Aguirre, M.J.; Muená, J.P.; Dehaen, W.; Maes, W.; Ngo, T.H.; Ramírez, G.; Arévalo, M.C. Electro-reduction of oxygen to water mediated by stable glassy carbon electrodes modified by Co(II)-porphyrins with voluminous meso-substituent. *Int. J. Electrochem. Sci.* **2015**, *10*, 3949.
40. Bard, A.J.; Faulkner, L.R. *Electrochemical Methods: Fundamentals and Applications*; Wiley: New York, NY, USA, 2000; ISBN 978-0-471-04372-0.
41. Ríos, R.; Marín, A.; Ramírez, G. Nitrite electro-oxidation mediated by Co(II)-[tetra(4-aminophenyl) porphyrin]-modified electrodes: Behavior as an amperometric sensor. *J. Coord. Chem.* **2010**, *63*, 1283–1294. [[CrossRef](#)]
42. Tham, M.K.; Walker, R.D.; Gubbins, K.E. Diffusion of Oxygen and Hydrogen in Aqueous Potassium Hydroxide Solutions. *J. Phys. Chem.* **1970**, *74*, 1747–1751. [[CrossRef](#)]
43. American Public Health Association (APHA); American Water Works Association (AWWA); Water Environment Federation (WEF). *Standard Methods for the Examination of Water and Wastewater*, 22nd ed.; United Book Press Inc.: Baltimore, MD, USA, 2012.
44. Andrieux, C.P.; Seavant, J.M. Heterogeneous versus homogeneous catalysis of electrochemical reactions. *J. Electroanal. Chem.* **1978**, *93*, 163–168. [[CrossRef](#)]
45. Srejc, I.; Rakocevic, Z.; Nenadovic, M.; Strbac, S. Oxygen reduction on polycrystalline palladium in acid and alkaline solutions: Topographical and chemical Pd surface changes. *Electrochim. Acta* **2015**, *169*, 22–31. [[CrossRef](#)]
46. Blizanac, B.; Ross, P.; Markovic, N. Oxygen Reduction on Silver Low-Index Single-Crystal Surfaces in Alkaline Solution: Rotating Ring Disk Ag(h kl) Studies. *J. Phys. Chem. B* **2006**, *110*, 4735–4741. [[CrossRef](#)] [[PubMed](#)]
47. Stamenkovic, V.; Schmidt, T.; Ross, P.; Markovic, N. Surface composition effects in electrocatalysis: Kinetics of oxygen reduction on well-defined Pt₃Ni and Pt₃Co alloy surfaces. *J. Phys. Chem. B* **2002**, *106*, 11970–11979. [[CrossRef](#)]
48. Zhao, Y.; Liu, J.; Zhao, Y.; Wang, F. Composition-Controlled Synthesis of Carbon-Supported Pt–Co Alloy Nanoparticles and Their Origin of the Activity Enhancement for Oxygen Reduction Reaction. *Phys. Chem. Chem. Phys.* **2014**, *16*, 19298–19306. [[CrossRef](#)] [[PubMed](#)]
49. Córdoba-Torres, P.; Mesquita, T.J.; Nogueira, R.P. Relationship between the origin of constant-phase element behavior in electrochemical impedance spectroscopy and electrode surface structure. *J. Phys. Chem. C* **2015**, *119*, 4136–4147. [[CrossRef](#)]
50. Wang, S.; Zhang, L.; Xia, Z.; Roy, A.; Chang, D.W.; Baek, J.B.; Dai, L. BCN Graphene as Efficient Metal-Free Electrocatalyst for the Oxygen Reduction Reaction. *Angew. Chem.* **2012**, *124*, 4285–4288. [[CrossRef](#)]
51. Luo, Z.; Lim, S.; Tian, Z.; Shang, J.; Lai, L.; MacDonald, B.; Fu, C.; Shen, Z.; Yu, T.; Lin, J. Pyridinic N doped graphene: Synthesis, electronic structure, and electrocatalytic property. *J. Mater. Chem.* **2011**, *21*, 8038–8044. [[CrossRef](#)]
52. Li, Y.; Zhao, Y.; Cheng, H.; Hu, Y.; Shi, G.; Dai, L.; Qu, L. Nitrogen-Doped Graphene Quantum Dots with Oxygen-Rich Functional Groups. *J. Am. Chem. Soc.* **2012**, *134*, 15–18. [[CrossRef](#)]
53. Jiang, L.; Cui, L.; He, X. Cobalt-porphyrin noncovalently functionalized graphene as nonprecious-metal electrocatalyst for oxygen reduction reaction in an alkaline medium. *J. Solid State Electrochem.* **2015**, *19*, 497–506. [[CrossRef](#)]
54. Gidi, L.; Canales, C.; Aguirre, M.J.; Armijo, F.; Ramírez, G. Four-Electron Reduction of Oxygen Electrocatalyzed by a Mixture of Porphyrin Complexes onto Glassy Carbon Electrode. *Int. J. Electrochem. Sci.* **2018**, *13*, 1666–1682. [[CrossRef](#)]

